




Correlated many-body noise and emergent $1/f$ behaviorP. N. Thomas Lloyd ^{1,2,*}, Valentin Walther ^{2,3} and H. R. Sadeghpour ²¹*Department of Physics, University of California, Santa Barbara, California 93106, USA*²*ITAMP, Center for Astrophysics|Harvard & Smithsonian, Cambridge, Massachusetts 02138, USA*³*Department of Physics, Harvard University, Cambridge, Massachusetts 02138, USA*

(Received 27 August 2021; accepted 21 December 2021; published 11 January 2022)

Fluctuating electric fields emanating from surfaces are a major possible source of decoherence in a number of quantum applications, including trapped ions and near-surface nitrogen-vacancy diamond qubits. Here, we show that at low temperatures, due to superradiant decay, phonon-induced excitation exchange between adsorbed atoms can counterintuitively mitigate the electric field noise. We derive an exact mapping between the noise spectrum of N interacting fluctuators with M vibrational levels to $\binom{N+M-1}{N}-1$ noninteracting two-level dipoles. The anharmonic interaction of the fluctuators with the surface is semiempirical and physically motivated. This anharmonicity affects the noise spectral power intensity at higher temperatures. We describe conditions for which the ubiquitous $1/f$ noise emerges naturally from the coupled dynamics of identical fluctuators and whose behavior depends critically on correlation among the fluctuators.

DOI: [10.1103/PhysRevA.105.L010402](https://doi.org/10.1103/PhysRevA.105.L010402)

Introduction. Electric field noise emanating from surfaces is a worrisome aspect limiting the duty cycles for a host of miniaturized applications in quantum physics [1–3]. Patch potentials—spatially variant electrostatic potentials on surfaces—affect force measurements of quantum electrodynamics or noncontact friction at short distances [4–6]. Surface electric field fluctuation is one of the largest contributors of noise at mHz (milli) frequencies for operation of space-based gravitational wave detectors [7]. Noise produced by fluctuating charges on diamond surfaces can even be more pernicious than magnetic noise for near-surface nitrogen-vacancy (NV) qubits [8–10]. Experiments have established that surface-induced low-frequency noise is a major source of decoherence in trapped ion qubit operations [11–13].

Identifying a single source of surface noise is a daunting challenge [14]. Nevertheless, there is growing evidence supported by microscopic and phenomenological theories and surface experiments to suggest that adsorbed impurities (“adatoms”) on surfaces are at work in generating fluctuating electric fields in ion traps, silicon cantilever tips, and NV-center diamonds [6,8,11,15–21]. No single behavior of anomalous noise in ion traps has been observed over the full range of temperatures [22–26] though noise tends to decrease at lower temperatures.

When the impurity concentration is high, correlated dynamics between impurity fluctuators can begin to dominate. In this Letter, we consider the effect of one such collective coupling on the noise spectral power, where the adsorbed fluctuating dipoles conspire to emit to and absorb from the same phonon mode. Coherent radiation has been of long-standing interest since Dicke’s seminal work demonstrating the enhanced radiance among correlated emitters [27,28].

We show that collective many-body decay leads to a reduction in noise intensity. We extend the usual two-level fluctuator paradigm to include the anharmonicity of levels and study the frequency and temperature influence of the anharmonic interaction on the noise power spectrum. By exploiting the symmetry properties of the phonon jump operators which determine the evolution of a Lindbladian master equation for N M -level fluctuators, we can make level-specific statements on how the noise emerges from the convolution of two-time correlators. The ubiquitous low-frequency $1/f$ noise emerges in this work due to the correlated dynamics of surface adsorbed dipoles when mutually independent patches are distributed with an adatom number as $1/N$. We show how this particular distribution emerges from the correlated dynamics in our derivation. This Letter constitutes a first-principles microscopic derivation of the $1/f$ noise and because the impurity-surface interaction is described within a potential landscape approach, the method is generally applicable over a wide range of adatom masses and vibrational frequencies. It can thus give rise to $1/f$ noise in the common MHz regime and at higher frequencies.

Interaction Hamiltonian and many-adatom master equation. A much studied possible source of noise in ion microtraps originates from impurity atoms that are adsorbed on metallic electrode surfaces. At large atom-surface separations, the surface potential is determined by the atomic dynamical polarization and is attractive, while repulsive forces dominate at short distances, where the adatom wave function overlaps with the surface.

This general binding is captured with an anharmonic potential, \exp^{-3} , $U(z) = \frac{\tilde{\beta}}{\tilde{\beta}-3} U_0 [\frac{3}{\tilde{\beta}} e^{\tilde{\beta}(1-z/z_0)} - (\frac{z_0}{z})^3]$, where U_0 is the potential depth at the equilibrium position z_0 . $\tilde{\beta} = \beta_0 z_0$, where β_0 is the reciprocal range of repulsion and z is the distance of the adatom from the surface [29,30]. The full

*ptlloyd@berkeley.edu

potential depends on the transverse (x, y) coordinates due to surface roughness and impurity mobility [31], but we take these contributions to average out or otherwise be weak on a metal surface where the electrons are smeared out. Thus, we only focus on motion normal to the surface. Each bound state of this potential is associated with a permanent dipole moment [17,32] and transitions between the states produce electric noise. Near z_0 the harmonic approximation holds and the fundamental overtone transition frequency can be written as $\omega_0 = \omega_{12} \approx \sqrt{\frac{3U_0(\beta^2 - 4\beta)}{mz_0^2(\beta - 3)}}$, where m is the adatom mass. We emphasize that most of the following work applies to a varied class of possible surface potentials [33,34].

We consider an ensemble of N adatoms interacting with the surface through M bound states, and described by a density matrix $\hat{\rho}$. A transition from level ν to μ ($E_\mu < E_\nu$) on atom n is described by the operator $\hat{b}_n^{\mu\nu} = |\mu\rangle\langle\nu|$ accompanied by the emission of a phonon into the bulk of frequency $\omega_{\mu\nu} = \omega_\nu - \omega_\mu$. Following similar arguments as those found in Refs. [35–39] for atom-photon coupling, we derive the master equation for our system [40]. We assume and validate the usual Markovian approximation that both correlations decay much faster than the correlation among the adatoms and that retardation effects can be ignored [41]. Under these conditions, we can solve for the cooperative decay $\Gamma_{mn}^{\mu\nu}$ and energy shift $\delta\omega_{m,n}$ and obtain an effective description for the correlated adatom ensemble, which we write in Lindbladian form

$$\partial_t \hat{\rho} = \sum_{\mu\nu}^M i[\hat{\rho}, \hat{\mathcal{H}}^{\mu\nu}] + \mathcal{L}^{\mu\nu}(\hat{\rho}), \quad (1)$$

with

$$\begin{aligned} \hat{\mathcal{H}}^{\mu\nu} &= \sum_{mn}^N \hat{b}_m^{\mu\nu\dagger} \hat{b}_n^{\mu\nu} (\omega_{\mu\nu} + \delta\omega_{mn}^{\mu\nu}), \\ \mathcal{L}^{\mu\nu}(\hat{\rho}) &= \sum_{mn}^N \frac{\Gamma_{mn}^{\mu\nu}}{1 - e^{-\beta\omega_{\mu\nu}}} \left[\hat{b}_m^{\mu\nu} \hat{\rho} \hat{b}_n^{\mu\nu\dagger} - \frac{1}{2} \{ \hat{b}_n^{\mu\nu\dagger} \hat{b}_m^{\mu\nu}, \hat{\rho} \} \right. \\ &\quad \left. + e^{-\beta\omega_{\mu\nu}} \left(\hat{b}_m^{\mu\nu\dagger} \hat{\rho} \hat{b}_n^{\mu\nu} - \frac{1}{2} \{ \hat{b}_n^{\mu\nu} \hat{b}_m^{\mu\nu\dagger}, \hat{\rho} \} \right) \right]. \quad (2) \end{aligned}$$

The Hamiltonian describes that a phonon after being emitted from an adatom transitioning from state ν to state μ can be absorbed by one of the other adatoms, promoting it from state μ to state ν . This is analogous to the exchange of virtual photons in dense multilevel atomic gases. The dissipative interaction of adatoms m and n in state μ and ν is given by the matrix $\Gamma_{mn}^{\mu\nu} = \frac{3}{2} \Gamma_0^{\mu\nu} f(k^{\mu\nu} r_{mn})$, where the level transition frequency is $\Gamma_0^{\mu\nu} = \frac{|\langle\mu|\nabla U|\nu\rangle|^2 \omega_{\mu\nu}}{2\pi\hbar c^3 \mathcal{N}}$ given that $k^{\mu\nu} = \frac{\omega_{\mu\nu}}{c}$, \mathcal{N} is the bulk density, and c is the phonon speed in the bulk. Both the coherent exchange process and the decay carry an intrinsic dependence on the distance of any pair of two adatoms, given by the function f [35]. In the long-wavelength limit, f is a constant. Thus we can safely remove the spatial dependence from consideration, but will return to it in the last section of the text. The inverse temperature, in units of frequency, is $\beta = T^{-1}$, where $T = k_b \mathcal{T} / \hbar$, with \mathcal{T} as the temperature in Kelvin. The quantity of merit in our derivations is $\beta\omega_0$, where ω_0 is the main transition frequency.

Adatom exchange symmetry. The interaction potential is harmonic about z_0 , and thus the approximate fundamental transition rate is $\Gamma_0 = \Gamma_0^{12} \approx \frac{1}{4\pi} \frac{\omega_0^4 m}{c^3 \mathcal{N}}$. This expression is useful in the $N > 1$ case since in the long-wavelength limit, where $k^{\mu\nu} r_{mn} \ll 1$, the decay is spatially independent such that $\Gamma_{mn}^{\mu\nu}$ becomes constant with elements, $\Gamma_0^{\mu\nu}$. In this limit, an emitted virtual phonon is equally likely to be absorbed by any of the adatoms, revealing that the system is fully symmetric under exchange of two adatoms.

All such transitions are captured by a collective operator $\hat{L}^{\mu\nu} = \sum_i^N \hat{b}_i^{\mu\nu}$ acting on all adatoms equally. This affords a particularly simple description, where we can naturally reduce Eq. (1) in the fully symmetric basis. Then the action of the fully symmetric operators strictly isolates the symmetric subspace from all other states [42,43]. We denote the symmetric states as $|m_1 m_2 \dots m_M\rangle$, where m_i , etc., indicates the number of atoms in level i with $N = \sum_i m_i$. The action of $L_{\mu\nu}$ on a state is given by $\hat{L}_{\mu\nu} | \dots, m_\mu, \dots, m_\nu, \dots \rangle = \sqrt{(m_\mu + 1)m_\nu} | \dots, m_\mu + 1, \dots, m_\nu - 1, \dots \rangle$. Furthermore, the evolution of populations in the symmetric basis are decoupled from coherences. Assuming an unexcited initial state, the system remains in the subspace spanned by $\binom{N+M-1}{N}$ populations of the symmetric subspace, denoted by ρ_{m_1, \dots, m_M} .

These populations are eigenstates of the Hamiltonian, which therefore does not contribute to the system evolution. This renders an effective classical model for the interacting adatoms. This is understood directly by expanding Eq. (1) in the symmetric population basis

$$\begin{aligned} \dot{\rho}_{m_1, \dots, m_M} &= \sum_{\mu, \nu} F^{\mu\nu} [G^{\nu\mu} \times (e^{-\beta\omega_{\mu\nu}} \rho_{\dots, m_\mu+1, \dots, m_\nu-1, \dots} - \rho_{m_1, \dots, m_M}) \\ &\quad + G^{\mu\nu} \times (\rho_{\dots, m_\mu-1, \dots, m_\nu+1, \dots} - e^{-\beta\omega_{\mu\nu}} \rho_{m_1, \dots, m_M})], \quad (3) \end{aligned}$$

where $F^{\mu\nu} = \frac{\Gamma_0^{\mu\nu}}{1 - e^{-\beta\omega_{\mu\nu}}}$ and $G^{\mu\nu} = m_\mu(m_\nu + 1)$. Equation (3) defines a linear matrix equation for the density matrix components, $\dot{\rho}_i = \sum_j M_{ij} \rho_j$, where ρ_j is the j th state in the symmetric basis we have described and M_{ij} is the transition element between two of the states. Now that we have a description for the dynamics of the vibrational states of our system, we can write an equation for the change in dipole moment. Choosing $\hat{\rho}_i = |i\rangle\langle i|$ as the projector of the symmetric state i , we can write the dipole operator of this state as $\hat{\mu}(t) = \sum_i D_i \hat{\rho}_i(t)$, where D_i is the associated dipole moment magnitude. This value is given by the sum over the dipole moments of the populated levels of the i th state weighted by their occupation (e.g., $\hat{\rho}_5 = |201\rangle\langle 201| \rightarrow D_5 = 2d_1 + d_3$).

Noise spectrum of correlated anharmonic fluctuators. We calculate the magnitude of the electric field noise by invoking the Wiener-Khinchin theorem [44,45], which in this context states that the electric field noise power spectrum is the Fourier transform of the autocorrelation function of $\hat{\mu}$,

$$S(\omega) = \int_{-\infty}^{\infty} d\tau [\langle \hat{\mu}(\tau) \hat{\mu}(0) \rangle - \langle \hat{\mu}(0) \rangle^2] e^{i\omega\tau}. \quad (4)$$

The correlation functions can be evaluated using the quantum regression theorem [46]. The first term in Eq. (4) can be written as $\langle \hat{\mu}(\tau) \hat{\mu}(0) \rangle = \sum_{i,j} D_i D_j \langle \hat{\rho}_i(\tau) \hat{\rho}_j(0) \rangle$. Since the operators ρ_i just represent projections, they

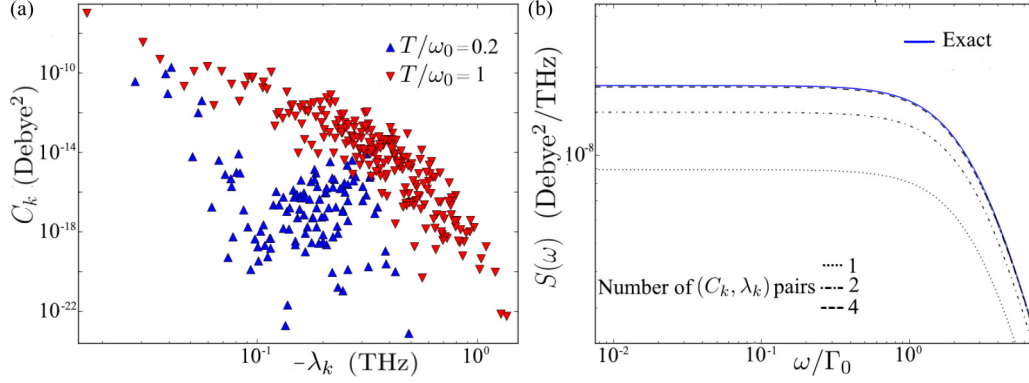


FIG. 1. (a) The coefficients C_k in Eq. (5) are shown as a function of eigenvalues λ_k for $N = 3$. The up (blue) and down (red) pointing triangles correspond to numerically exact calculations at $T/\omega_0 = 0.2, 1$, respectively. The widespread distributions of weights C_k over ten orders of magnitude suggest an approximation scheme utilizing the largest C_k . (b) The noise power spectrum illustrates the point: With only the highest weighted (C_k, λ_k) pairs, here up to four pairs, results converge to the exact values for $T/\omega_0 = 0.2$. The convergence will only be more rapid for higher temperatures. Here, we chose $U_0 = 0.6$ eV, $m = 100$ amu, $\beta_0 = 1.86 \text{ \AA}^{-1}$, and $z_0 = 3.1 \text{ \AA}$ as an example of a tightly bound adatom species. We note that qualitatively similar results are obtained for weakly bound adatoms, where the noise spectrum is shifted to lower frequencies.

satisfy the same equation of motion as the density matrix $\partial_t \langle \hat{\rho}_i(\tau) \hat{\rho}_j(0) \rangle = \sum_j M_{ij} \langle \hat{\rho}_j(\tau) \hat{\rho}_j(0) \rangle$. As the matrix is diagonalizable, $M = A^{-1} \mathcal{O} A$ with eigenvalues $\{\lambda_k \leq 0\}$, a particularly simple solution is in terms of the eigenmodes $\langle \hat{\rho}_i(\tau) \hat{\rho}_j(0) \rangle = \sum_k A_{ik}^{-1} \sum_l A_{kl} \langle \hat{\rho}_l(\tau) \hat{\rho}_j(0) \rangle e^{\lambda_k \tau}$. The first term in Eq. (4) can thus be written as $\langle \hat{\mu}(\tau) \hat{\mu}(0) \rangle = \sum_{i,j} D_i D_j \sum_k A_{ik}^{-1} \sum_l A_{kl} \langle \hat{\rho}_l(0) \hat{\rho}_j(0) \rangle e^{\lambda_k \tau}$. Note that the term $\lambda_k = 0$ corresponds to the steady state and can be simplified into $\langle \hat{\mu}(0) \hat{\mu}(0) \rangle$, canceling the second term in Eq. (4) as expected. We further note that the projector can be simplified into the steady-state value $\langle \hat{\rho}_i(0) \hat{\rho}_j(0) \rangle = \langle \hat{\rho}_j(0) \rangle \delta_{ij} = \rho_j(0)^{\text{ss}} \delta_{ij}$. The Fourier integral can now be performed analytically, when observing the time symmetry of the correlator $\langle \hat{\mu}(\tau) \hat{\mu}(0) \rangle = \langle \hat{\mu}(-\tau) \hat{\mu}(0) \rangle$ in the steady state,

$$\begin{aligned} S(\omega) &= \sum_{i,j} D_i D_j \sum_{k \setminus \{\lambda_k=0\}} A_{ik}^{-1} A_{kj} \rho_j(0)^{\text{ss}} \int_{-\infty}^{\infty} d\tau e^{\lambda_k |\tau|} e^{i\omega \tau} \\ &= - \sum_{i,j} D_i D_j \sum_{k \setminus \{\lambda_k=0\}} A_{ik}^{-1} A_{kj} \rho_j(0)^{\text{ss}} \frac{2\lambda_k}{\lambda_k^2 + \omega^2}, \end{aligned}$$

where the integral converges because $\lambda_k < 0$. For the same reason, the noise spectrum is strictly positive definite. A concise interpretation can be obtained by defining $C_k = 2 \sum_{i,j} D_i D_j A_{ik}^{-1} A_{kj} \rho_j(0)^{\text{ss}}$ such that the noise spectrum becomes a sum of Lorentzians

$$S(\omega) = \sum_{k \setminus \{\lambda_k=0\}} C_k \frac{-\lambda_k}{\lambda_k^2 + \omega^2}. \quad (5)$$

This simple exact solution expresses the remarkable equivalence of the electric field noise from an N -body correlated system to that of $\binom{N+M-1}{N} - 1$ (the number of states excluding the steady state) independent effective two-level fluctuators. In this picture, each fluctuator has a weight C_k with an effective lifetime $\tau_k = \lambda_k^{-1}$. This provides a natural order of decay that is useful for a simplified analysis of noise spectra at high and low frequencies.

Correlated noise. The impurity-surface interaction potential, transition energies $\Gamma_{\mu\nu}$, dipole moments d_μ ,

transition rate constants $\Gamma_{\mu\nu}$, and temperature T define our surface-fluctuator system. Numerical calculations indicate that d_μ decreases with increasing vibrational level while $\Gamma^{\mu\mu+1}$ peaks at some intermediate level [40]. Figure 1(a) displays the decomposition of terms in Eq. (5) at the example of a tightly bound adatom species. Each component λ corresponds to a Lorentzian noise profile. While it is evident that many Lorentzians contribute at both low and high temperatures, only a few λ terms dominate the noise power spectrum decomposition. The effect on the noise power spectrum is shown in Fig. 1(b), where the sum of only a few λ terms are necessary to reproduce the converged numerical results (calculations converge with $M = 10$), reaffirming the expectation that the level population is thermally activated and determined by the Boltzmann factor $\mathcal{T} = e^{-\beta\omega_0}$. At low temperatures $T/\omega_0 < 1$, transitions occur near the harmonic minimum z_0 such that only the lowest two states are dominant. The noise spectrum can be expanded perturbatively in powers of \mathcal{T} ,

$$S_N(\omega) = 2(d_1 - d_2)^2 \frac{N\Gamma_0}{(N\Gamma_0)^2 + \omega^2} \mathcal{T} + O(\mathcal{T}^2). \quad (6)$$

An immediate observation, in comparing to Eq. (5), is $\lambda = N\Gamma_0$. This proportionality of the eigenvalues with N is exploited below to describe how the ubiquitous $1/f$ noise emerges. The equivalent coefficients C_k are independent of N . The frequency-independent white noise magnitude per adatom, $\frac{1}{N} S_N(\omega = 0)$, now scales as $\frac{1}{N^2}$, as observed in Fig. 2(b). This suggests that at low temperatures, correlated phonon transitions conspire to suppress electric field noise [see Fig. 2(a)]. In this regime, a larger number of adatoms not only decreases the noise per adatom but, in fact, decreases the total noise of N adatoms to a value lower than that of a single adatom ($N = 1$). This is a reasonably surprising consequence of superradiant decay applied to noisy adatoms on surfaces.

Superradiant decay. Figure 2(a) displays the noise spectrum for three different temperatures. We recover the superradiant behavior at low temperatures as discussed above, where the overall low-frequency noise is attenuated. This

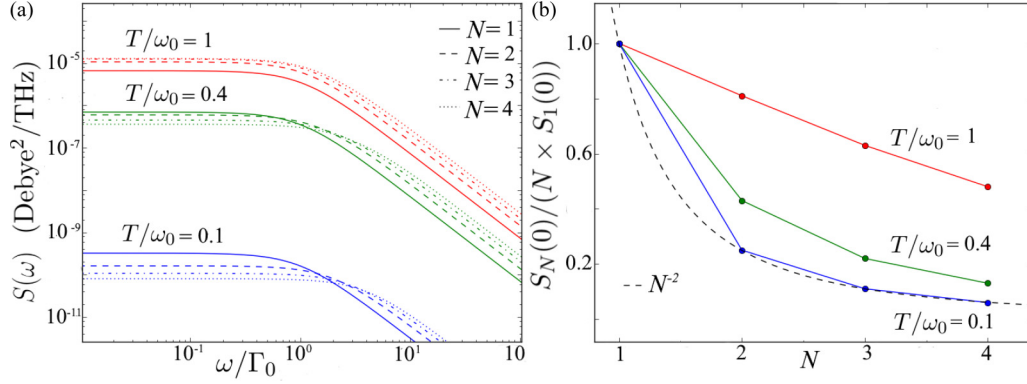


FIG. 2. The noise spectral function for adatoms of mass $m = 100$ amu interacting with the surface potential at depth $U_0 = 250$ meV at $T/\omega_0 = 0.1, 0.4$, and 1 with β_0 and z_0 as before. (a) The correlated noise spectrum is shown for different patch sizes N . At $T/\omega_0 < 1$, correlated superradiant decay results in a lowering of the white noise with an increasing number of correlated adatoms N . Thus, in this regime one adatom is a larger source of noise than two or more correlated adatoms. With $T/\omega_0 \sim 1$, superradiant decay does not prevent an increasing noise magnitude as a function of increasing N . (b) The magnitude of the white noise spectra per adatom at different T/ω_0 is shown to decrease with increasing N where in the low-temperature limit the N^{-2} scaling appears as predicted by Eq. (6). The solid lines are guides for the eye.

effect is weakened at intermediate temperatures and eventually reversed, and the total noise increases with increasing N . Remarkably, the noise per adatom generally remains suppressed as seen in Fig. 2(b). At higher temperatures, the influence of the interaction potential anharmonicity on the level structure and transition rate constants (see below) increases. As analyzed in Fig. 1, the contribution of different (λ_k, C_k) sets to Eq. (6) shifts such that at $\omega/(N\Gamma_0) \approx 1$, the spectral dependence turns over from constant to $1/f^2$. Throughout, we remain at temperatures such that the adatom does not detach from the surface via thermal fluctuations.

Anharmonicity. For rising temperatures the anharmonic behavior of the model potential will have an observable influence on the noise power spectrum. At $T/\omega_0 = 0.2$, the dominant effective two-level fluctuator approximates the exact white noise spectrum to within a few percent. At higher temperatures more and more bound states contribute, a process we illustrate here by considering the next-to-leading order in the expansion in \mathcal{T} in Eq. (6). A parametric measure of anharmonicity is found by expanding $U(z)$ about z_0 to the third order in z , such that the frequency asymmetry between level spacing is $\delta = \omega_0 - \omega_{23}$. With increasing N , the spectral density of the \mathcal{T}^2 contribution $C_2(N, \delta)$ plateaus, but with increasing δ , the plateau heights also increase [40].

Emergent $1/f$ noise. The overall noise originates from the mesoscopic scale and randomly scattered impurities with differing local densities which together define a surface coverage. The interaction with the phonon hub is therefore given by the separation of all adatom pairs. Instead of reintroducing this spatial dependence, we provide an insightful approximation of this complex system by segregating the surface into patches, whose adatoms are fully correlated, while each patch interacts independently with the phonon hub. Thus, the noise power spectrum can be approximated as a weighted sum of the patches of size N , $S_{\text{tot}}(\omega) = \sum_{N=1}^{N_{\text{max}}} \mathcal{D}(N) S_N(\omega)$ with a corresponding relative weight factor $\mathcal{D}(N)$.

In particular, at low temperatures the noise spectrum can be written as $S_N(\omega) = \mathcal{C} \frac{N\Gamma_0}{(N\Gamma_0)^2 + \omega^2}$, where \mathcal{C} are the coefficients of the Lorentzian in Eq. (6). Since \mathcal{C} has no N dependence, it can be moved out of the sum and normalized. Next, we consider a

distribution whereby each patch is weighted by $\mathcal{D}(N) = N^{-1}$, as a heuristic model where the relative frequency of small patches is high and that of large patches is low.

Then,

$$\lim_{N_{\text{max}} \rightarrow \infty} S_{\text{tot}}(\omega) = \frac{\mathcal{C}}{2} \left(-\frac{\Gamma_0}{\omega^2} + \frac{\pi \coth\left(\frac{\pi\omega}{\Gamma_0}\right)}{\omega} \right). \quad (7)$$

The noise thus shows a universal frequency dependence set by the fundamental transition rate Γ_0 . At small frequencies, $\omega/\Gamma_0 \ll 1$, the noise thus approaches a constant value $\pi^2/(6\Gamma_0)$ while $1/f$ behavior emerges for $\omega/\Gamma_0 > 1$ (see Fig. 3). For a finite number of adatoms in a patch, the spectral behavior shows $1/f$ noise across a finite frequency range, before returning to the typical $1/f^2$ behavior at the highest frequencies.

This derivation is complimentary to the phenomenological derivation of $1/f$ noise by Dutta and Horn [47]. There, it is demonstrated that the noise of thermally activated two-level

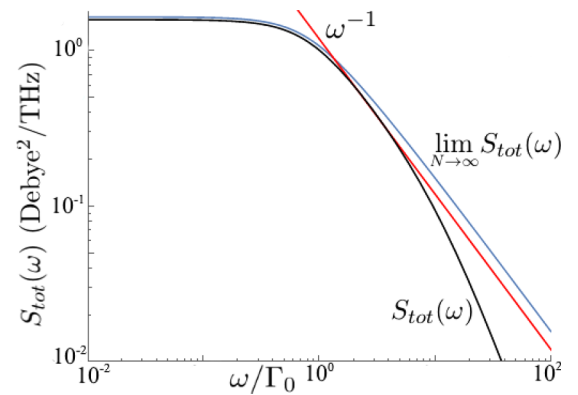


FIG. 3. The emergence of $1/f$ noise with a $\mathcal{D}(N) = \frac{1}{N}$ patch distribution. The black bottommost curve results from a sum over $N_{\text{max}} = 10$ correlated adatoms in $S_{\text{tot}}(\omega)$ while the blue curve is the $N_{\text{max}} \rightarrow \infty$ limit in Eq. (7). The latter has a universal functional form in ω/Γ_0 . With increasing numbers of correlated adatoms in each patch, the noise spectrum turns from $1/f^2$ to $1/f$.

fluctuators is of $1/f$ type in a given frequency range if their energy distribution within and well beyond that frequency range is constant. The underlying physical reason is that the associated lifetimes τ are then distributed as $\mathcal{D}(\tau) \propto \tau^{-1}$. Here, due to superradiant decay, each patch has a characteristic timescale $\tau_N \sim \frac{1}{\Gamma_0 N}$; larger patches have faster dynamics and therefore shorter decay timescales (less noise). This offers an alternative origin for the emergence of the distribution $D(\tau) \propto \tau^{-1}$ for the assumed distribution of patch sizes. Thus, we provide a physical derivation for the ubiquitous $1/f$ noise that does not depend on *a priori* assumptions on an assumed energy level distribution and emerges naturally from the coupled dynamics as a discrete sum over a distribution of identical fluctuators. At higher T/ω_0 , level multiplicity and interaction anharmonicity will enter, as discussed above. We note that a linear relationship between the dominant λ_k and N exists at higher temperatures, suggesting that a key ingredient for our description of $1/f$ emergence persists beyond Eq. (6) [40].

Realization. The appearance of correlated dynamics depends on the adatom species, specific surface interaction, and impurity density. Correlated dynamics will generally emerge when the dominant phonon wavelength exceeds the typically adatom-adatom separation, i.e., $\mathcal{C} \equiv \sqrt{\mathcal{R}}(2\pi c/\omega_0) \gtrsim 1$, where c is the phonon speed in the material. Such conditions tend to be satisfied in ion traps with a large adatom concentration of relatively massive adatoms or molecules, whose surface vibrational energies $\hbar\omega_0$ are low. These energies may vary from 1 eV for a hydrogen adatom to 1 meV for loosely bound heavy adatoms [17,29,48,49]. For instance, argon or xenon impurities on a gold surface ($c \approx 3240$ m/s) have vibrational energies $\hbar\omega_0 \sim 1\text{--}5$ meV [50,51], such that $\mathcal{C} > 1$ for moderate densities $\mathcal{R} > 10^{-3} \text{ \AA}^{-2}$. The superradiant suppression of electric field noise is expected in such systems at $\mathcal{T} < 50$ K, i.e., $\beta\omega_0 \gg 1$. Noise magnitudes for these parameters vary from 10^{-14} to $10^{-9} \text{ V}^2 \text{ m}^{-2} \text{ THz}^{-1}$ [40]. More reactive adatoms such as carbon, nitrogen, or oxygen, typical contaminant species, can possess higher binding energies and thus $\hbar\omega_0 \gtrsim 10$ meV, therefore reaching the correlated regime at greater densities, $\mathcal{R} \sim 5 \times 10^{-3} \text{ \AA}^{-2}$. With $\Gamma_0 \approx \frac{1}{4\pi} \frac{\omega_0^4 m}{c^3 \mathcal{N}}$ for masses typical of physisorbed species, such as rare-gas atoms, and $\omega_0 \sim 1$ THz, Γ_0 ranges from 1 to 100 MHz. For chemisorbed species which are more tightly bound to the surface, the condition $\mathcal{C} \gtrsim 1$ is met at higher temperatures

and larger Γ_0 . We emphasize that this theoretical framework makes no assumption on operating conditions and can thus generally be applied.

Concluding remarks and outlook. Superradiant decay, caused by the collective emission into and absorption from a phonon bath, can suppress the electric field noise emanating from N fluctuating impurities on surfaces. The electric field noise of this N -body correlated system maps to $\binom{N+M-1}{N}$ -1 independent effective two-level fluctuators. This is facilitated by exploiting the inherent permutation symmetry of adatoms at close distances. We further find that the correlated dynamics of N adatoms in surface patches with relative frequencies $1/N$ results in the ubiquitous $1/f$ noise spectrum.

Future extensions of this correlated model for noise suppression can account for impurity diffusion and exchange of adatoms between patches. Care is then necessary to allow for spatial dependence of the phonon dynamics and the possible population of states without perfect permutation symmetry. This more complex scenario may allow the emergence of robust $1/f$ noise for a wider class of particle distributions than considered in the present Letter. Another promising direction lies in the regime of high temperatures. Interesting features at these temperatures can already be seen in Fig. 1, where the equivalent two-level fluctuators are distributed in a more regular fashion than at low temperatures. Moreover, a single Lorentzian tends to dominate more with increasing temperature, requiring fewer pairings of (C_k, λ_k) for a converged description of the noise spectrum. This suggests a possible way in which the otherwise more complex computations at higher-temperature calculations could be simplified. However, a comprehensive model needs to account for the possible thermal ejection of adatoms at high temperatures. A recent work [19] compliments this work with detailed numerical simulations of specific adsorbates on a gold surface and similarly comes to the conclusion that correlated dynamics is crucial for the emergence of $1/f$ noise.

Acknowledgments. We acknowledge several helpful discussions with Arghavan Safavi-Naini and use of her notes in the early stages of this work. P.N.T.L. thanks ITAMP for the opportunity to visit where these calculations began, and a virtual summer internship. This work has been supported by the NSF through a grant for the Institute for Theoretical Atomic, Molecular, and Optical Physics at Harvard University and the Smithsonian Astrophysical Observatory.

-
- [1] F. Arute, K. Arya, R. Babbush, D. Bacon, J. C. Bardin, R. Barends, R. Biswas, S. Boixo, F. G. S. L. Brandao, D. A. Buell, B. Burkett, Y. Chen, Z. Chen, B. Chiaro, R. Collins, W. Courtney, A. Dunsworth, E. Farhi, B. Foxen, A. Fowler *et al.*, *Nature (London)* **574**, 505 (2019).
 - [2] E. Paladino, Y. M. Galperin, G. Falci, and B. L. Altshuler, *Rev. Mod. Phys.* **86**, 361 (2014).
 - [3] J. A. Sedlacek, E. Kim, S. T. Rittenhouse, P. F. Weck, H. R. Sadeghpour, and J. P. Shaffer, *Phys. Rev. Lett.* **116**, 133201 (2016).
 - [4] S. K. Lamoreaux, *Phys. Rev. Lett.* **78**, 5 (1997).
 - [5] B. C. Stipe, H. J. Mamin, T. D. Stowe, T. W. Kenny, and D. Rugar, *Phys. Rev. Lett.* **87**, 096801 (2001).
 - [6] S. Kuehn, R. F. Loring, and J. A. Marohn, *Phys. Rev. Lett.* **96**, 156103 (2006).
 - [7] S. E. Pollack, S. Schlamminger, and J. H. Gundlach, *Phys. Rev. Lett.* **101**, 071101 (2008).
 - [8] M. Kim, H. J. Mamin, M. H. Sherwood, K. Ohno, D. D. Awschalom, and D. Rugar, *Phys. Rev. Lett.* **115**, 087602 (2015).
 - [9] Y. Romach, C. Müller, T. Unden, L. J. Rogers, T. Isoda, K. M. Itoh, M. Markham, A. Stacey, J. Meijer, S. Pezzagna, B. Naydenov, L. P. McGuinness, N. Bar-Gill, and F. Jelezko, *Phys. Rev. Lett.* **114**, 017601 (2015).
 - [10] B. A. Myers, A. Ariyaratne, and A. C. B. Jayich, *Phys. Rev. Lett.* **118**, 197201 (2017).

- [11] D. A. Hite, Y. Colombe, A. C. Wilson, K. R. Brown, U. Warring, R. Jördens, J. D. Jost, K. S. McKay, D. P. Pappas, D. Leibfried, and D. J. Wineland, *Phys. Rev. Lett.* **109**, 103001 (2012).
- [12] D. A. Hite, K. S. McKay, S. Kotler, D. Leibfried, D. J. Wineland, and D. P. Pappas, *MRS Adv.* **2**, 2189 (2017).
- [13] M. Cetina, L. N. Egan, C. A. Noel, M. L. Goldman, A. R. Risinger, D. Zhu, D. Biswas, and C. Monroe, [arXiv:2007.06768](https://arxiv.org/abs/2007.06768).
- [14] M. Brownnutt, M. Kumph, P. Rabl, and R. Blatt, *Rev. Mod. Phys.* **87**, 1419 (2015).
- [15] C. Henkel and B. Horowitz, *Phys. Rev. A* **78**, 042902 (2008).
- [16] Q. A. Turchette, Kielpinski, B. E. King, D. Leibfried, D. M. Meekhof, C. J. Myatt, M. A. Rowe, C. A. Sackett, C. S. Wood, W. M. Itano, C. Monroe, and D. J. Wineland, *Phys. Rev. A* **61**, 063418 (2000).
- [17] A. Safavi-Naini, P. Rabl, P. F. Weck, and H. R. Sadeghpour, *Phys. Rev. A* **84**, 023412 (2011).
- [18] J. A. Sedlacek, J. Stuart, D. H. Slichter, C. D. Bruzewicz, R. McConnell, J. M. Sage, and J. Chiaverini, *Phys. Rev. A* **98**, 063430 (2018).
- [19] B. Foulon, K. G. Ray, C. E. Kim, Y. Liu, B. M. Rubenstein, and V. Lordi, [arXiv:2107.01177](https://arxiv.org/abs/2107.01177).
- [20] P. Chrostoski, H. R. Sadeghpour, and D. H. Santamore, *Phys. Rev. Appl.* **10**, 064056 (2018).
- [21] H. J. Mamin, M. Kim, M. H. Sherwood, C. T. Rettner, K. Ohno, D. D. Awschalom, and D. Rugar, *Science* **339**, 557 (2013).
- [22] J. Labaziewicz, Y. Ge, D. R. Leibbrandt, S. X. Wang, R. Shewmon, and I. L. Chuang, *Phys. Rev. Lett.* **101**, 180602 (2008).
- [23] J. Chiaverini and J. M. Sage, *Phys. Rev. A* **89**, 012318 (2014).
- [24] N. Daniilidis, S. Gerber, G. Bolloten, M. Ramm, A. Ransford, E. Ulin-Avila, I. Talukdar, and H. Häffner, *Phys. Rev. B* **89**, 245435 (2014).
- [25] M. Berlin-Udi, C. Matthiesen, P. N. T. Lloyd, A. Alonso, C. Noel, C. Orme, C. E. Kim, V. Lordi, and H. Häffner, [arXiv:2103.04482](https://arxiv.org/abs/2103.04482).
- [26] C. Noel, M. Berlin-Udi, C. Matthiesen, J. Yu, Y. Zhou, V. Lordi, and H. Häffner, *Phys. Rev. A* **99**, 063427 (2019).
- [27] R. H. Dicke, *Phys. Rev.* **93**, 99 (1954).
- [28] M. Gross and S. Haroche, *Phys. Rep.* **93**, 301 (1982).
- [29] H. Hoinke, *Rev. Mod. Phys.* **52**, 933 (1980).
- [30] R. A. Buckingham, *Proc. R. Soc. London* **168**, 264 (1938).
- [31] K. G. Ray, B. M. Rubenstein, W. Gu, and V. Lordi, *New J. Phys.* **21**, 053043 (2019).
- [32] P. R. Antoniewicz, *Phys. Rev. Lett.* **32**, 1424 (1974).
- [33] G. H. Low, P. F. Herskind, and I. L. Chuang, *Phys. Rev. A* **84**, 053425 (2011).
- [34] J. L. Garrett, J. Kim, and J. N. Munday, *Phys. Rev. Research* **2**, 023355 (2020).
- [35] C. Gardiner and P. Zoller, *The Quantum World of Ultra-Cold Atoms and Light Book II: Foundations of Quantum Optics* (Imperial College Press, London, 2014).
- [36] W. Schäfer and M. Wegener, *Semiconductor Optics and Transport Phenomena* (Springer, Berlin, 2002).
- [37] R. J. Bettles, Cooperative interactions in lattices of atomic dipoles, Ph.D. thesis, Durham University, 2016.
- [38] R. H. Lehmburg, *Phys. Rev. A* **2**, 883 (1970).
- [39] R. H. Lehmburg, *Phys. Rev. A* **2**, 889 (1970).
- [40] See Supplemental Material at <http://link.aps.org/supplemental/10.1103/PhysRevA.105.L010402> for more details on the master equation, anharmonicity, elevated temperature, and noise magnitude.
- [41] M. T. Manzoni, M. Moreno-Cardoner, A. Asenjo-Garcia, J. V. Porto, A. V. Gorshkov, and D. E. Chang, *New J. Phys.* **20**, 083048 (2018).
- [42] Y. Zhang, Y. X. Zhang, and K. Mølmer, *New J. Phys.* **20**, 112001 (2018).
- [43] B. Q. Baragiola, B. A. Chase, and J. M. Geremia, *Phys. Rev. A* **81**, 032104 (2010).
- [44] N. Wiener, *Acta Math.* **55**, 117 (1930).
- [45] A. Khintchine, *Math. Ann.* **109**, 604 (1934).
- [46] C. Gardiner and P. Zoller, *The Quantum World of Ultra-Cold Atoms and Light Book I: Foundations of Quantum Optics* (Imperial College Press, London, 2014).
- [47] P. Dutta and P. M. Horn, *Rev. Mod. Phys.* **53**, 497 (1981).
- [48] Y. Santiago-Rodríguez, J. A. Herron, M. C. Curet-Arana, and M. Mavrikakis, *Surf. Sci.* **627**, 57 (2014).
- [49] K. Oura, V. G. Lifshits, A. A. Saranin, A. V. Zotov, and M. Katayama, *Surface Science: An Introduction* (Springer, Berlin, 2003).
- [50] S. Ossicini, *Phys. Rev. B* **33**, 873 (1986).
- [51] J. L. F. Da Silva and C. Stampfl, *Phys. Rev. B* **77**, 045401 (2008).